

## Simultaneous Adsorption of Chromium (VI) and Phosphate by Calcined Mg-Al-CO<sub>3</sub> Layered Double Hydroxides

Xiulan Song\* and Yuhong Wu

College of Environmental Science and Engineering, Taiyuan University of Technology, No. 79 Yingze West Street, Taiyuan 030024, Shanxi, P.R. China. \*E-mail: xlsong123@163.com  
Received January 17, 2014, Accepted February 27, 2014

The adsorption characteristics of chromium (VI) and phosphate on calcined Mg-Al-CO<sub>3</sub> layered double hydroxides (CLDH) were investigated in single and binary systems. A series of batch experiments were performed to study the influence of various experimental parameters. In this study, CLDH exhibited a high adsorption capacity for Cr (VI) and P in a single system. The experimental data were close to the theoretical adsorption capacity given by the Langmuir isotherm, the calculating adsorption capacities of Cr (VI) and P were up to 70.42 mg/g and 97.09 mg/g, respectively. It was found that the initial pH was approximately 6 and it took 24 h to reach equilibrium when P and Cr (VI) were added simultaneously. The experimental data were best fitted by a pseudo-second-order kinetics model. Competitive adsorption between Cr (VI) and P existed in the binary system. The presence of Cr (VI) had no significant influence on P adsorption. However, the suppression of Cr (VI) adsorption was obvious when the initial concentration of P was up to 10 mg/L with a concentration of 0.5 g/L of CLDH.

**Key Words :** Chromium, Phosphate, Layered double hydroxides

### Introduction

Chromium (Cr) is a major pollutant in wastewater, and it can be found generally in rocks, soil, plants, animals, and gases.<sup>1,2</sup> The most common oxidation states of chromium are Cr (III) and Cr (VI). Cr (VI) is one of the most dangerous heavy metals because of its strong oxidizability and high toxicity.<sup>3-5</sup> As is known Cr (VI) is mainly released to the environment by textile processing, leather tanning, mining operations, water-cooling, electroplating and pigment manufacturing,<sup>6-8</sup> which may cause environmental and health problems. The recommended limit of Cr (VI) in drinking water is 0.05 mg/L.<sup>2,9,10</sup> Methods for the removal of Cr (VI) involve chemical precipitation, electrolysis, biochemical process, and adsorption.<sup>11,12</sup> Phosphorus is one of the major nutrients for plant growth and it comes from agricultural fertilisers, soaps, and detergents with formulations containing sodium tripolyphosphates, atmospheric nitrogen, erosion of soils containing nutrients, and discharge from sewage treatment plants.<sup>7,13</sup> Though it is an essential macronutrient responsible for healthy plant growth, concentration in an excess of the described limit can result in the eutrophication of lakes, rivers, and seas.<sup>14-16</sup> The permissible limit for phosphate in drinking water is only 1.0 mg/L.<sup>7</sup> Therefore, high concentrations of phosphate (P) must be removed from wastewater before its discharge.<sup>17</sup> There are also numerous methods used for removing phosphate, such as: chemical precipitation, biological processes, adsorption, and crystallization.<sup>15</sup>

With the rapid development of industrialisation and urbanisation in recent years, large amounts of Cr (VI) and P were produced in wastewater. Compared to their permissible

limits, industrial and agricultural effluents contain much higher concentrations of Cr (VI) and P. These substances will adversely affect the quality of water and soil: they pose a significant threat to environmental security. To mitigate the adverse effects of P, an appropriate removal technology is required. A wide range of physical and chemical processes is available to eliminate Cr (VI) and P from wastewater, such as: liquid-liquid extraction, hybrid anion exchange-precipitation,<sup>10,18,19</sup> and adsorption.<sup>7,16</sup> Among these potential separation technologies, adsorption is one of the most promising because of its initially low cost, flexibility, and ease of operation.<sup>20-24</sup> So the search for ideal adsorbents with high adsorption capacity becomes necessary.

Layered double hydroxides (LDH) are considered one of the most promising inorganic functional materials, due to their special layered structure, large surface area and low-cost. Their general formula can be normally expressed as  $M^{2+}_{1-x}M^{3+}_x(OH)_2(A^{n-}_{x/n}) \cdot mH_2O$ , where  $M^{2+}$  and  $M^{3+}$  are divalent and trivalent metal cations that occupy octahedral sites in the hydroxide layers,  $A^{n-}$  is an exchangeable anion located in the interlayer space between two hydroxide layers. The  $CO_3^{2-}$  anion is generally the interlayer anion,<sup>10</sup> the interlayered  $CO_3^{2-}$  anion can be removed by calcining at a certain temperature.<sup>25</sup> The calcined layered double hydroxides (CLDH) can be rehydrated in water. During their rehydration, the layered hydroxide structure is reconstructed with the incorporation of anions from the solution.<sup>9</sup> This is the so-called "memory effect". LDH plays an important role in medicine, pesticides, biological material science, *etc.* In recent years, the applications of LDH have been extended to the environmental sciences. With high anion exchange capacity and a large surface area, LDH was successfully

used as an adsorbent in water treatment. Moreover, the calcined layered double hydroxides compound was found to be a better adsorbent as, because of its memory effect, it express high adsorptive capacity of dyes,  $\text{ClO}_4^-$ ,  $\text{F}^-$ , etc.<sup>26-28</sup> However, most studies focus on the adsorption of a single pollutant, there are hardly any reports on the performance of these compounds when used for simultaneous removal of Cr (VI) and P.

In this work, the authors attempt to develop such adsorbent materials of calcined Mg-Al- $\text{CO}_3$  LDH (CLDH) for the simultaneous removal of Cr (VI) and phosphate, investigate the influencing factors (contact time, solution pH, and initial anion concentrations), isotherm and kinetic modelling of competitive adsorption, and provide a detailed analysis of Cr (VI) and P adsorption characteristics on CLDH. The adsorption mechanism was important when predicting the adsorption process of various anions.

### Experimental

**Preparation of Materials.** CLDH was synthesised by a co-precipitation method.  $\text{Mg}(\text{NO}_3)_2 \cdot 6\text{H}_2\text{O}$  (25.6 g) and  $\text{Al}(\text{NO}_3)_3 \cdot 9\text{H}_2\text{O}$  (18.75 g) were dissolved in deionised water (Solution A). Solution B was prepared by dissolving NaOH (20 g) in deionised water. Solution A and Solution B were added to an  $\text{Na}_2\text{CO}_3$  solution at a rate of 5 mL/min under constant stirring, and the mixed solution was maintained at a constant pH by NaOH and  $\text{HNO}_3$ . The mixture was stirred for 30 min after addition. The precipitate thus obtained was aged at 80 °C for 18 h. Subsequently, it was washed out with deionised water to remove nitrate and sodium ions and filtered. Then the wet solid was dried at 80 °C for 12 h to separate the Mg-Al- $\text{CO}_3$  LDH. CLDH was obtained by calcining the Mg-Al- $\text{CO}_3$  LDH at 350 °C for 5 h.

**Sample Characterisation.** The CLDH samples before and after the adsorption of P and Cr(VI) ions were examined by X-ray diffraction (XRD) and Fourier transform infrared (FTIR) spectroscopy. XRD patterns were recorded on a Rigaku D/Max-2500 diffraction at a scan rate of 8°/min with  $\text{CuK}\alpha$  radiation, using a voltage of 40 kV and a current of 30 mA over the range  $5^\circ \leq 2\theta \leq 65^\circ$ . FTIR spectra were recorded on a Thermo-Nicolet Nexus 670 FTIR spectrometer in the KBr phase over the wave number range: 400 to 4000  $\text{cm}^{-1}$ .

**Adsorption Assays.** Chromium (VI) and P stock solution were prepared by dissolving  $\text{K}_2\text{Cr}_2\text{O}_7$  and  $\text{KH}_2\text{PO}_4$  in deionised water, respectively. All adsorption experiments were carried out in a temperature controlled shaker using shaking flasks containing Cr (VI) and P solution with different initial concentrations for a predetermined contact time at 150 rpm. The effects of contact time were recorded at specific time intervals with initial concentrations of 40 mg/L at 30 °C with 100 mg adsorbent and 200 mL solution. The influence of initial solution pH was investigated over the range  $3 \leq \text{pH} \leq 11$ . The pH was adjusted by 0.2 mol/L NaOH and 0.2 mol/L  $\text{HNO}_3$  at a concentration of Cr (VI) or P of 40 mg/L. Adsorption isotherms were evaluated at 30 °C and 50

mg of sorbent was immersed into 100 mL of solution (from 20 to 80 mg/L) with constant agitation.

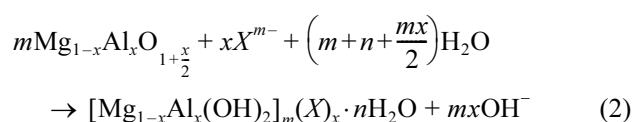
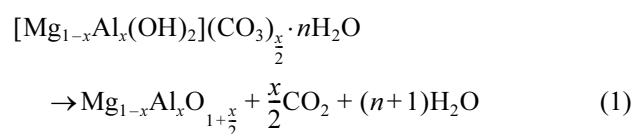
Water samples were filtered for analysis of the concentrations of residual Cr (VI) and P solution. The concentration of P in the solution was determined by molybdate blue method, which was obtained by colorimetric reading of a spectrophotometer at a wavelength of 700 nm. The concentration of Cr (VI) in aqueous solution was determined spectrophotometrically at 540 nm, following the diphenylcarbazide method. The amount of Cr (VI) and P adsorbed was calculated by the difference between the initial and final concentrations. The adsorption capacity  $q_e$  (mg/g) was calculated as follows:

$$q_e = (C_0 - C_e)V/m \quad (1)$$

where  $C_0$  (mg/L) and  $C_e$  (mg/L) are the initial and equilibrium concentrations of Cr(VI) or P respectively,  $V$  (L) is the solution volume and  $m$  (g) the mass of the adsorbent.

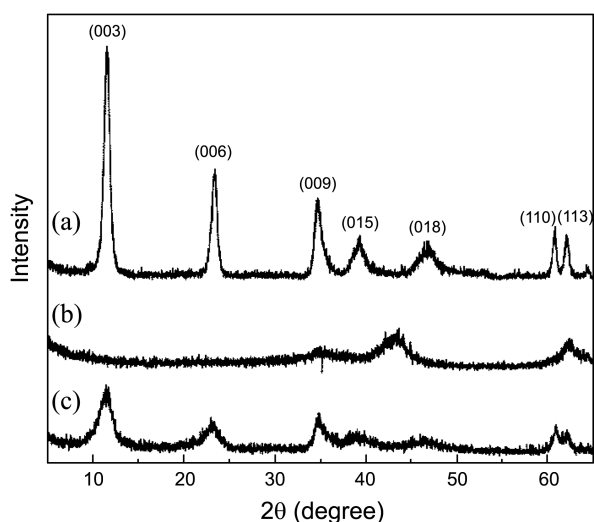
### Results and Discussion

**Characterisation.** Figure 1 shows XRD patterns of Mg-Al- $\text{CO}_3$  LDH, CLDH, CLDH after adsorption of Cr (VI) and P ions. The XRD patterns of Mg-Al- $\text{CO}_3$  LDH (curve (a) in Fig. 1) exhibited the characteristic peaks of hydrotalcite-like compounds. The strong X-ray reflection represented a high degree of crystallinity and a layered structure in the samples. After calcining at 350 °C, the well-defined diffraction peaks disappeared (curve (b) in Fig. 1), thus indicating that the hydrotalcite-like structure had collapsed and there was a disordering within the stacking of the layers.<sup>29</sup> Furthermore, the broad peaks were attributed to the formation of Mg-Al mixed oxides. In the current column test, it is assumed that CLDH can adsorb ions *via* three mechanisms: (i) electrostatic attraction on surface, (ii) ion exchange interaction between anions and hydroxyl ions, (iii) regeneration of its initial layered structure, as expressed by the following reaction:<sup>29,30</sup>



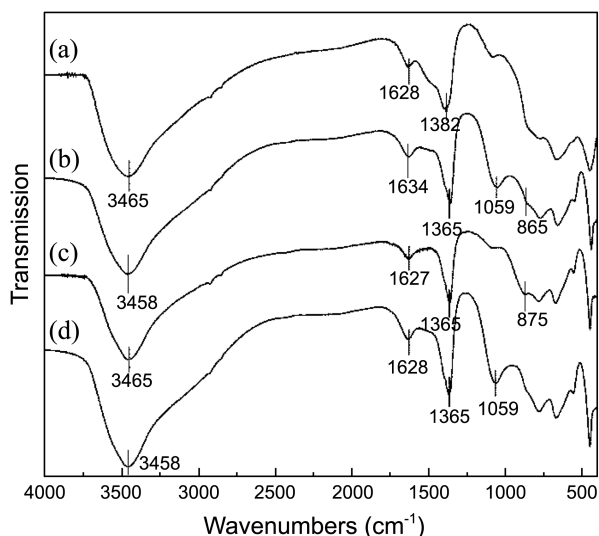
XRD patterns of CLDH after adsorption of Cr(VI) and phosphate (curves (c) and (d) in Fig. 1) regained their LDH characteristic reflections, such as (003) and (006), which demonstrated that the hydrotalcite structure was regenerated by intercalation of Cr(VI) and P ions into the interlayer region, this further indicated the existence of the claimed “memory effect”.

Figure 2 showed the FTIR spectra of the chosen samples: Mg-Al- $\text{CO}_3$  LDH, CLDH after adsorption of Cr (VI), CLDH



**Figure 1.** XRD patterns of (a) Mg-Al-CO<sub>3</sub> LDH, (b) Mg-Al-CO<sub>3</sub> LDH calcined at 350 °C, (c) CLDH after adsorption of Cr(VI) and P.

after adsorption of P, and CLDH after adsorption of Cr (VI) and phosphate. A high intensity band centered on *c.* 3460 cm<sup>-1</sup> was observed, which could be attributed to the stretching vibration of O-H bonds in metal hydroxides and water molecules.<sup>20,31</sup> The band appearing at *c.* 1628 cm<sup>-1</sup> revealed the O-H bending mode of the water molecules. The bands revealed the presence of hydroxyl ions arising from the brucite-like layers. The band at *c.* 1360 cm<sup>-1</sup> was attributed to the characteristic vibrations of carbonate groups. The result demonstrated that carbonate was not completely removed after calcining at 350 °C and that there was a strong affinity between carbonate and LDH. After adsorption, the band at *c.* 1060 cm<sup>-1</sup> (curves (b) and (d) in Fig. 2) indicated the presence of phosphate intercalated in the interlayer space of CLDH,<sup>32</sup> and the band at 800 to 950 cm<sup>-1</sup> (curves (b) and (c) in Fig. 2) corresponded to the characteristic vibration of



**Figure 2.** FTIR spectra of (a) Mg-Al-CO<sub>3</sub> LDHs calcined at 350 °C, (b) CLDH after adsorption of Cr(VI) and P, (c) CLDH after adsorption of Cr(VI), (d) CLDH after adsorption of P.

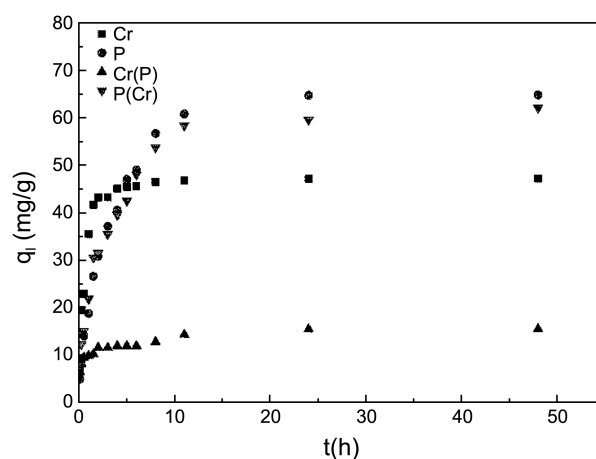


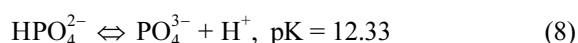
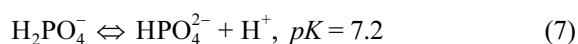
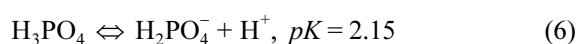
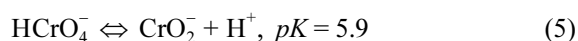
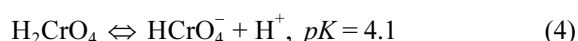
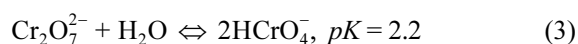
**Figure 3.** Effect of contact time on Cr (VI) and P adsorption by CLDH ( $C_{0(P)} = 40$  mg/L and  $C_{0(Cr)} = 40$  mg/L, adsorbent dosage 0.5 g/L, temperature  $30 \pm 0.2$  °C).

Cr (VI).<sup>30</sup> The FTIR spectra did not show such a strong absorbance intensity of Cr (VI), when P and Cr (VI) were simultaneously adsorbed by CLDH, which demonstrated that the presence of P decreased the adsorption of Cr (VI) and competitive adsorption between P and Cr (VI) occurred.

**Effect of Contact Time.** To confirm the equilibration time for the adsorption of Cr (VI) and P and to discuss the adsorption kinetics, the contact times of Cr (VI) and P adsorbed by CLDH in single and binary system were investigated. Figure 3 shows plots of the time *versus* the amount of Cr (VI) and P adsorbed: the adsorption of Cr (VI) and P in the single system initially increased with time and then gradually reached the equilibrium. We can also see that the adsorption of Cr (VI) onto CLDH in the single system was comparatively faster and it reached a plateau in approximately 4 h. Since equilibrium was reached in less than 24 h, an equilibrium time of 24 h was applied to the subsequent experiments. Figure 3 indicated that the adsorption capacity of Cr (VI) in a single system was larger than that in a binary system, which demonstrated that the presence of P decreased the adsorption of Cr (VI) on CLDH. This result agreed with the FTIR spectral data. The adsorbed Cr (VI) onto CLDH decreased in binary system may be due to competition for the same adsorption sites with P. However, the existence of Cr (VI) had no effect on P adsorption. CLDH may have had a greater affinity for P than Cr (VI).

**Effect of Initial pH.** The pH of the solution controlled the surface change of the adsorbent and the speciation of ions, so it is considered to be an important parameter which affects the adsorption.<sup>10</sup> As shown in Figure 4, the adsorption of P and Cr (VI) on CLDH was investigated at different initial pH values ranging from 3.0 to 11.0 with a constant ionic density. From Figure 4, it was seen that the adsorption capacity of Cr (VI) and P increased with the increase in previous pH. The highest Cr (VI) adsorption by CLDH was found at a pH of 6.0, P adsorption reached its maximum at a pH of 5.0. Herein, a pH of 6.0 was chosen as ideal for the present study considering the fact that below this pH the

adsorbent may be unstable.<sup>29</sup> With further increase in pH, there was an apparent decrease in the adsorption of Cr (VI) and P. It was suggested that a high pH value was unfavourable to the adsorption. These results could be attributed to the excessive amount of hydroxyl ions, which can compete for active sites in the adsorption process with Cr (VI) and P. Meanwhile, a high pH will encourage the formation of negative ions on the adsorbent surface. It would produce a repulsive interaction between the adsorbent and ions in solution.<sup>29</sup> Besides, the modification of pH can cause the formation of multivalent chromium species ( $\text{Cr}_2\text{O}_7^{2-}$ ,  $\text{HCrO}_4^-$ ,  $\text{CrO}_4^{2-}$ ) and phosphate species ( $\text{H}_2\text{PO}_4^-$ ,  $\text{HPO}_4^{2-}$ ,  $\text{PO}_4^{3-}$ ):



According to Eq. (2), as the speciation of multivalent anions changed with the solution pH, adsorbing the same amount of anions required more adsorbents, which led to a reduction in Cr (VI) and P sorption at higher pH values. Such as, adsorbing the same amount of P, multivalent  $\text{HPO}_4^{2-}$  demanded CLDH two times more than monovalent  $\text{H}_2\text{PO}_4^-$  did.

It should be noted that the sorption capacity of Cr (VI) and P decreased after the mixture of additional ions, and the change was greater for Cr (VI) than for P. It was suggested that competitive adsorption between Cr (VI) and P occurred. It also implied that the adsorption of Cr (VI) decreased to a great degree in the presence of P, but the existence of Cr (VI) had little effect on the adsorption of P. The P was able to be interacted with CLDH much more easily than Cr (VI) did. It

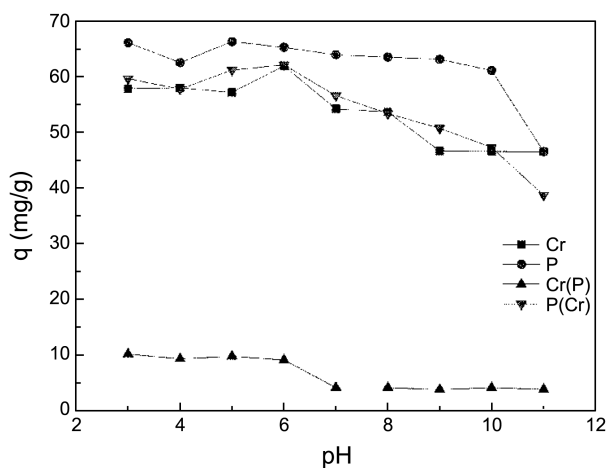


**Figure 4.** Effect of pH on Cr (VI) and P adsorption by CLDH ( $C_{0(P)} = 40 \text{ mg/L}$  and  $C_{0(\text{Cr})} = 40 \text{ mg/L}$ , adsorbent dosage  $0.5 \text{ g/L}$ , adsorption time  $24 \text{ h}$ , temperature  $30 \pm 0.2 \text{ }^\circ\text{C}$ ).

**Table 1.** Langmuir and Freundlich isotherm model constants and correlation coefficients for adsorption of Cr (VI) and P on CLDH

ions	Langmuir isotherm			Freundlich isotherm		
	$q_m$ (mg/g)	$K_a$ (mg/L)	$R^2$	$n$	$K_b$	$R^2$
Cr	70.42	0.23	0.991	4.98	30.15	0.985
P	97.09	0.70	0.993	5.99	51.91	0.947
Cr(P)	68.49	0.01	0.606	1.40	1.42	0.938
P(Cr)	96.15	0.37	0.98	9.54	55.71	0.854

was difficult to be replaced by Cr (VI), once P was adsorbed on CLDH previously. In other words, CLDH may have had a stronger affinity for P compared to that possessed by Cr (VI).

**Measure of Adsorption Isotherm.** The adsorption isotherms of Cr (VI) and P are shown in Figure 5. Adsorption isotherms were used to determine the sorption capabilities and mechanisms of Cr (VI) or P by CLDH. The Langmuir and Freundlich models are often used to describe adsorption isotherms.

The Langmuir isotherm assumes monolayer coverage and all sites on solid surface have equal affinity for adsorbate molecules. It is expressed as:<sup>25</sup>

$$q_e = \frac{q_m K_a C_e}{1 + K_a C_e} \quad (9)$$

where  $q_e$  is the amount of anions adsorbed per unit mass of adsorbent at equilibrium (mg/g),  $q_m$  is the theoretical saturated adsorption capacity (mg/g),  $C_e$  is the equilibrium concentration of the anions in solution (mg/L),  $K_a$  is a Langmuir constant related to the adsorption-desorption energy and to the affinity of binding sites for anions (L/mg). The equation above can be rearranged to the following linear form:

$$\frac{C_e}{q_e} = \frac{1}{q_m K_a} + \frac{C_e}{q_m} \quad (10)$$

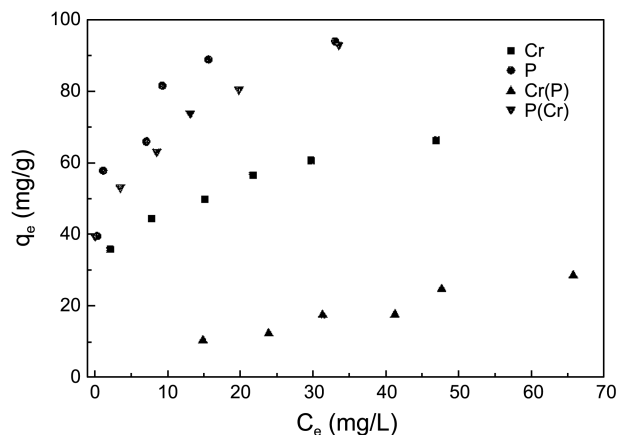


**Figure 5.** Adsorption isotherms of Cr (VI) and P by CLDH (adsorbent dosage  $0.5 \text{ g/L}$ , adsorption time  $24 \text{ h}$ , temperature  $30 \pm 0.2 \text{ }^\circ\text{C}$ ).

The linear form can be used for linearization of experimental data by plotting  $C_e/q_e$  versus  $C_e$  as shown in Figure 6. The constants  $q_m$  and  $K_a$  were determined from the slope and intercept of the plot and are presented in Table 1. The essential features of the isotherm can be expressed in terms of a dimensionless constant ( $R_L$ ) defined by:<sup>33</sup>

$$R_L = \frac{1}{1 + K_a C_0} \quad (11)$$

where  $C_0$  is the initial concentration of the anions. It is reported that:  $R_L = 0$  indicates irreversible adsorption,  $0 \leq R_L \leq 1$  indicates favourable adsorption, and when  $R_L > 1$ , the adsorption is unfavourable. It could be inferred here that for  $K_a > 0$ , adsorption was favourable.

The Freundlich isotherm was applied to non-ideal sorption on heterogeneous surfaces and multilayer adsorption, this empirical model was widely used and can be expressed by:<sup>29,34</sup>

$$q_e = K_b C_e^{1/n} \quad (12)$$

where  $K_b$  and  $n$  are the Freundlich constants incorporating all parameters affecting the adsorption process. It is reported that  $1 \leq n \leq 10$  represent favourable adsorption conditions. To determine the constants  $K_b$  and  $n$ , the Freundlich equation can be rearranged to its linear form:

$$\ln q_e = \ln K_b + \frac{1}{n} \ln C_e \quad (13)$$

Figure 7 shows the linear plot of the Freundlich isotherm of Cr (VI) and phosphate adsorption on CLDH at 30 °C.

Comparing the two isotherm models described above, the Langmuir isotherm was the most suitable for the characterisation of Cr (VI) or P adsorption behaviour and the experimental data were consistent with the Langmuir equation except Cr (VI) in binary system. It was found that CLDH showed a high capacity to sorb Cr (VI) or P. The maximum adsorption capacities of Cr (VI) or P in single system were up to 70.42 mg/g and 97.09 mg/g, respectively. The calculated  $K_a$  has positive values, which suggested that it was a

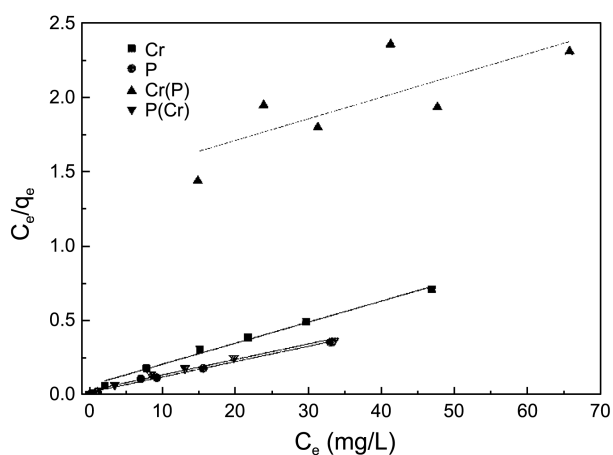


Figure 6. Linearized Langmuir isotherm plots of Cr (VI) and P adsorption by CLDH at 30 ± 0.2 °C.

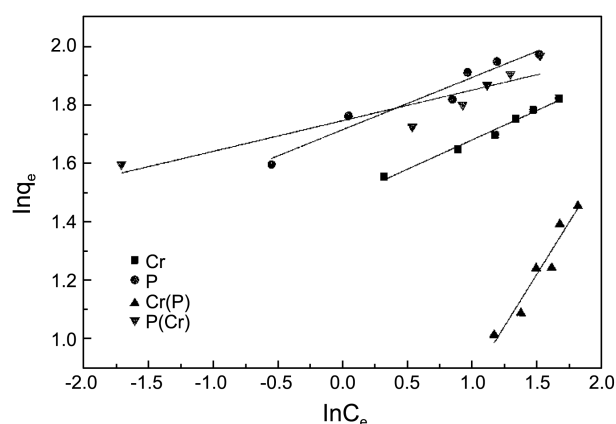


Figure 7. Linearized Freundlich isotherm plots of Cr (VI) and P adsorption by CLDH at 30 ± 0.2 °C.

favourable adsorption of Cr (VI) or P. The Freundlich model also gave a good fit to the adsorption behaviour. For Cr (VI) in binary system, the higher  $R^2$  values indicated the application of Freundlich isotherm. In addition, the values of  $n$  larger than 1 indicated a good sorption process of Cr (VI) or P on CLDH.

**Measure of Adsorption Kinetics.** To describe the sorption behaviour and its variation with contact time, several adsorption kinetic experiments for the simultaneous removal of Cr (VI) and P by CLDH were undertaken. Four kinetic models were used for this analysis of the sorption kinetics.<sup>27,35</sup>

The Lagergren's equation for pseudo first-order kinetics can be written as follows:

$$q_t = q_e(1 - e^{-K_1 t}) \quad (14)$$

where  $q_e$  denotes the amount of adsorbate adsorbed at equilibrium (mg/g),  $q_t$  is the amount of adsorbate adsorbed at reaction time  $t$  (mg/g), and  $K_1$  is the rate constant ( $\text{h}^{-1}$ ). Lagergren's first-order rate constant ( $K_1$ ) and  $q_e$  were calculated from the intercept and slope of the plot (Fig. 8) and are listed in Table 2 along with the corresponding correlation coefficients. It was observed that the calculated

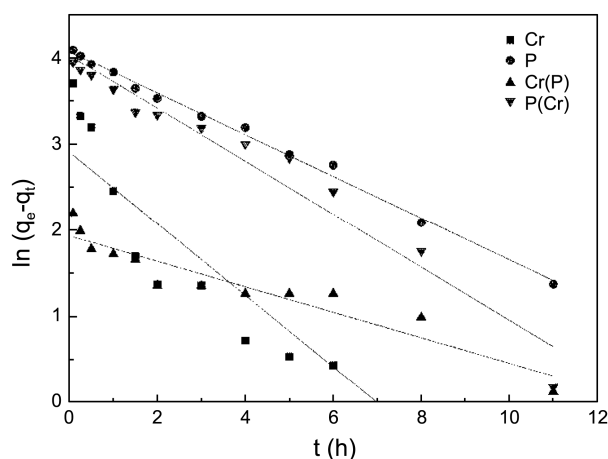


Figure 8. Pseudo-first-order model for adsorption of Cr (VI) and P by CLDH.

**Table 2.** Comparison between adsorption kinetic parameters of pseudo first-order, pseudo-second-order, Elovich equation and inter-particle diffusion models

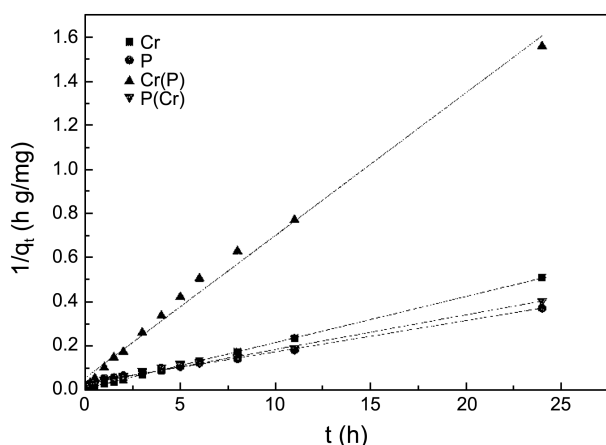
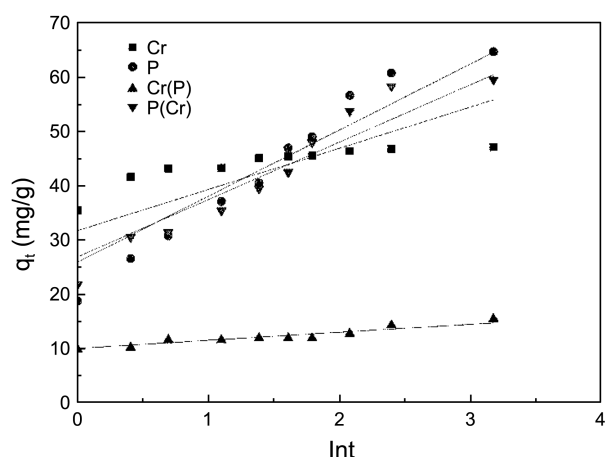
Adsorption kinetics	Constant	Ions			
		P	Cr	P(Cr)	Cr(P)
Pseudo-first-order model	$K_1$	0.24	0.54	0.31	0.15
	$q_e$	58.68	23.05	56.18	6.90
	$R^2$	0.995	0.861	0.956	0.891
Pseudo-second-order model	$K_2$	0.006	0.06	0.009	0.08
	$q_e$	70.92	48.08	63.69	15.48
	$R^2$	0.994	1	0.992	0.992
Elovich model	$\alpha$	102.44	496.4	134.44	1297.98
	$\beta$	0.082	0.13	0.01	0.68
	$R^2$	0.946	0.871	0.947	0.96
Intra-particle diffusion model	$K_i$	7.37	14.67	7.37	1.76
	$C$	7.61	12.73	11.18	7.83
	$R^2$	0.532	0.892	0.532	0.883

$q_e$  values did not agree with the experimental  $q_e$  values, suggesting that the adsorption of Cr (VI) and P on CLDH did not follow pseudo first-order kinetics.

The pseudo second-order model was established on the basis of the assumption that the occupation rate of adsorption sites was proportional to the square of the number of unoccupied sites as represented by:<sup>36</sup>

$$\frac{t}{q_t} = \frac{1}{K_2 q_e^2} + \frac{t}{q_e} \quad (15)$$

where  $q_t$  and  $q_e$  are the adsorption capacity at time  $t$  and equilibrium, respectively;  $k_2$  is the pseudo-second-order rate constant. The pseudo second-order kinetic at 30 °C is plotted in Figure 9;  $k_2$  and  $q_e$  calculated from the model are also listed in Table 2 along with the corresponding correlation coefficient. The predicted equilibrium uptakes were close to the experimental values indicating the applicability of the pseudo second-order model. The corresponding correlation coefficient  $R^2$  ( $> 0.99$ ) indicated that the pseudo second-order model could describe the adsorption of Cr (VI) and P.

**Figure 9.** Pseudo-second-order model for adsorption of Cr (VI) and P by CLDH.**Figure 10.** Elovich model for adsorption of Cr (VI) and P by CLDH.

The Elovich equation is given by:<sup>27</sup>

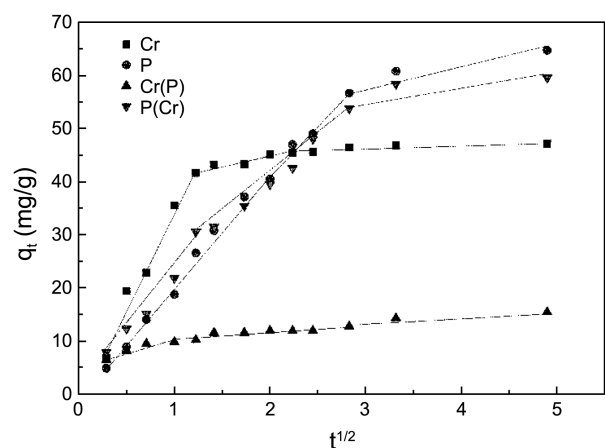
$$q_t = \beta \ln(\alpha\beta) + \beta \ln t \quad (16)$$

where  $\alpha$  is the initial sorption rate (mg/g) and  $\beta$  is related to the extent of surface coverage (g/mg). The calculated data are presented in Figure 10 and Table 2. The Elovich equation accounted for the characteristics of heterogeneous sorption sites. Since there were both external surface adsorption and interlayer ion exchange for CLDH adsorption, this may have resulted in a heterogeneous sorption process.<sup>35</sup>

To investigate the contribution of intra-particle behaviour on the adsorption process, the rate constant for intra-particle diffusion can be calculated from the following equation:<sup>27,29</sup>

$$q_t = K_i t^{1/2} + C \quad (17)$$

where  $K_i$  is the intra-particle diffusion rate constant (mg/g h<sup>1/2</sup>), and  $C$  is the vertical axis intercept. If the plot of  $q_t$  against  $t^{1/2}$  were linear, the adsorption process was deemed to have been determined by the intra-particle diffusion step. Additionally, intra-particle diffusion was the only rate-limiting step if the line tended to pass through the origin. Nevertheless, if the line revealed multi-linear facets, the

**Figure 11.** Intra-particle diffusion model for adsorption of Cr (VI) and P by CLDH.

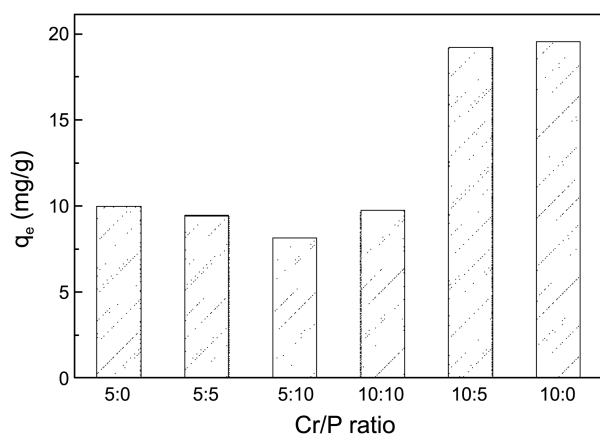


**Figure 12.** Adsorption capability of Cr (VI) before and after dosing with different Cr/P ratio.

adsorption process was deemed to have been complicated with more than one rate-limiting step in the sorption process. As shown in Table 2, the correlation coefficient indicated a lack of fit with the intra-particle model. The plot presented multi-linearity in Figure 11, indicating that the adsorption of Cr (VI) and P were complex and proceeded in different steps such as: (a) boundary layer diffusion, (b) particle surface adsorption, and (c) intra-particle diffusion.

**Effect of Initial Concentration of Cr (VI) and P.** Different adsorption performances of CLDH for Cr (VI) and P were observed when they co-existed compared to single systems, and the results are shown in Figures 12 and 13. With an initial Cr (VI) concentration of 5 mg/L and 10 mg/L, compared with the P removal capability of CLDH before dosing with P, the effect of subsequent addition of P with concentrations of 5 mg/L on the Cr (VI) removal could be ignored. However, when the P concentration was increased to up to 10 mg/L, the negative effect of P became more obvious, and the Cr (VI) removal capacity decreased by 18.7% and 49.2%, respectively. With initial P concentrations of 5 mg/L and 10 mg/L, the effects of the addition of Cr (VI) at concentrations of 5 and 10 mg/L on the P removal were negligible.

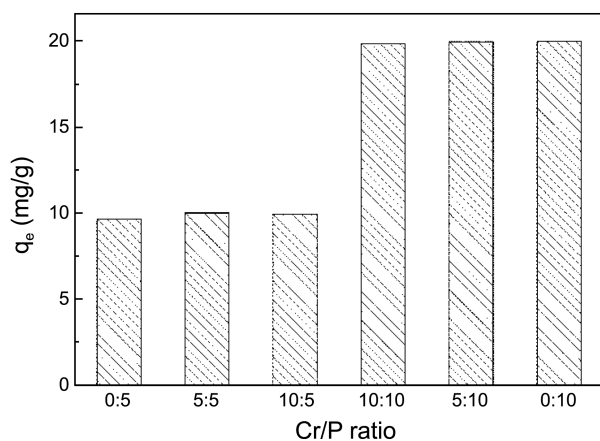


**Figure 13.** Adsorption capability of P before and after dosing with different Cr/P ratio.

These results suggested that the Cr (VI) and P removal capability of CLDH cannot be effected by the co-existence of Cr (VI) and P with an initial phosphate concentration of 5 mg/L, indicating that the CLDH adsorbents could achieve the simultaneous removal of Cr (VI) and P from an aqueous solution with an initial P concentration of approximately 5 mg/L.

## Conclusions

The adsorption of Cr (VI) and P on CLDH was investigated. The CLDH was effective in its ability to remove Cr (VI) and P in a single system. The adsorption isotherm results were described by the Langmuir and Freundlich models, and the constants  $K_a > 0$  and  $n > 1$  were indicative of favourable adsorption conditions. It was found that the optimum pH was approximately 6 and it took 24 h to reach equilibrium when Cr (VI) and P were added simultaneously. The adsorption process could be described by a pseudo second-order model.

Competitive adsorption between Cr (VI) and P existed in the binary system. P showed a stronger affinity with CLDH compared to that manifested by Cr (VI). The suppression of Cr (VI) adsorption was more obvious at P concentrations of up to 10 mg/L with a concentration of 0.5 g/L of CLDH. The XRD and FTIR results demonstrated the rehydration of mixed metal oxides and intercalation of Cr (VI) and P ions into the layer to reconstruct the hydroxide-like structure. The main adsorption mechanism of CLDH for Cr (VI) and P involved adsorption on the surface and the reconstruction of the original layered structure.

**Acknowledgments.** This work was supported by the Social Development and Technological Projects Fund of Shanxi Province (Grant no. 20100311125). We are grateful to the staff in their experimental facilities for providing us with the necessary equipment.

## References

- Mor, S.; Ravindra, K.; Bishnoi, N. R. *Bioresour. Technol.* **2007**, *98*(4), 954-957.
- Rodrigues, L. A.; Maschio, L. J.; da Silva, R. E.; da Caetano, M. L.; da Silva, P. *J. Hazard Mater.* **2010**, *173*(1-3), 630-636.
- Kotaš, J.; Stasicka, Z. *Environ. Pollut.* **2000**, *107*(3), 263-283.
- Pantsar-Kallio, M.; Reinikainen, S.; Oksanen, M. *Anal. Chim. Acta* **2001**, *439*(1), 9-17.
- Ramos-Ramírez, E.; Ortega, N. L. G.; Soto, C. A. C.; Gutiérrez, M. T. O. *J. Hazard Mater.* **2009**, *172*(2-3), 1527-1531.
- Zhou, J. B.; Wu, P. X.; Dang, Z.; Zhu, N. W.; Ping, L.; Wu, J. H.; Wang, X. D. *Chem. Eng. J.* **2010**, *162*(3), 1035-1044.
- Nthumbi, R. M.; Ngila, J. C.; Moodley, B.; Kindness, A.; Petrik, L. *Phys. Chem. Earth* **2012**, *50*-52, 243-251.
- Wang, S. W.; Tang, Y. P.; Tao, S. R. *Adsorption* **2008**, *14*, 823-830.
- Baran, A.; Bicak, E.; Baysal, S. H.; Önal, S. *Bioresour. Technol.* **2006**, *98*(3), 661-665.
- Wang, X. H.; Liu, F. F.; Lu, L.; Yang, S.; Zhao, Y.; Sun, L. B.; Wang, S. G. *Colloids Surf., A* **2013**, *423*, 42-49.
- Gao, H.; Liu, Y. G.; Zeng, G. M.; Xu, W. H.; Li, T.; Xia, W. B. *J.*

- Hazard Mater.* **2008**, 150(2), 446-452.
12. Yalçın, S.; Apak, R.; Hizal, J.; Afşar, H. *Sep. Sci. Technol.* **2001**, 36(10), 2181-2196.
13. Cloern, J. E. *Mar. Ecol. Prog. Ser.* **2001**, 210, 223-253.
14. Bell, P. R. F. *Water Res.* **1992**, 26(5), 553-568.
15. Das, J.; Patra, B. S.; Baliarsingh, N.; Parida, K. M. *Appl. Clay Sci.* **2006**, 32(3-4), 252-260.
16. Xu, X.; Gao, B. Y.; Tan, X.; Yue, Q. Y.; Zhong, Q. Q.; Li, Q. *Carbohydr. Polym.* **2011**, 84(3), 1054-1060.
17. Neal, C.; Jarvie, H. P.; Howarth, S. M.; Whitehead, P. G.; Williams, R. J.; Neal, M.; Harrow, M.; Wickham, H. *Sci. Total. Environ.* **2000**, 251-252, 477-496.
18. Ertul, S.; Bayrakci, M.; Yilmaz, M. *J. Hazard. Mater.* **2010**, 181(1-3), 1059-1065.
19. Qian, G. R.; Feng, L. L.; Zhou, J. Z.; Xu, Y. F.; Liu, J. Y.; Zang, J.; Xu, Z. P. *Chem. Eng. J.* **2012**, 181-182, 251-258.
20. Cheng, X.; Ye, J. X.; Sun, D. Z.; Chen, A. Y. *Chin. J. Chem. Eng.* **2011**, 19(3), 391-396.
21. Deng, H.; Yu, X. L. *Chem. Eng. J.* **2012**, 184, 205-212.
22. Ghosh, P. K. *J. Hazard. Mater.* **2009**, 171(1-3), 116-122.
23. He, S.; Zhao, Y. F.; Wei, M.; Evans, D. G.; Duan, X. *Ind. Eng. Chem. Res.* **2012**, 51(1), 285-291.
24. Namasivayam, C.; Sangeetha, D. *J. Colloid Interface Sci.* **2004**, 280(2), 359-365.
25. Cai, P.; Zheng, H.; Wang, C.; Ma, H. W.; Hu, J. C.; Pu, Y. B.; Liang, P. *J. Hazard. Mater.* **2012**, 213-214, 100-108.
26. Despoina, A. D.; Triantafyllidis, K. S.; Lazaridis, N. K.; Matis, K. A. *J. Chem. Technol. Biotechnol.* **2011**, 87(4), 575-582.
27. Yang, Y. Q.; Gao, N. Y.; Chu, W. H.; Zhang, Y. J.; Ma, Y. *J. Hazard. Mater.* **2012**, 209-210, 318-325.
28. Ma, W.; Zhao, N. N.; Yang, G.; Tian, L. Y.; Wang, R. *Desalination* **2011**, 268(1-3), 20-26.
29. Kang, D. J.; Yu, X. L.; Tong, S. R.; Ge, M. F.; Zuo, J. C.; Cao, C. Y.; Song, W. G. *Chem. Eng. J.* **2013**, 228, 731-740.
30. Xu, Y. F.; Zhang, J.; Qian, G. R.; Ren, Z.; Xu, Z. P.; Wu, Y. Y.; Liu, Q.; Qiao, S. Z. *Ind. Eng. Chem. Res.* **2010**, 49(6), 2752-2758.
31. Fernández, J. M.; Ulibarri, M. A.; Labajos, F. M.; Rives, V. J. *Mater. Chem.* **1998**, 8(11), 2507-2514.
32. Yin, L.; Lei, G. Y.; Li, C. J.; Liu, Z. J. *Environ. Chem.* **2012**, 31(7), 1049-1056 (in Chinese).
33. Otero, R.; Fernández, J. M.; González, M. A.; Pavlovic, I.; Ulibarri, M. A. *Chem. Eng. J.* **2013**, 221, 214-221.
34. Halajnia, A.; Oustan, S.; Najafi, N.; Khataee, A. R.; Lakzian, A. *Appl. Clay Sci.* **2013**, 80-81, 305-312.
35. Goh, K. H.; Lim, T. T. *J. Hazard. Mater.* **2010**, 180(1-3), 401-408.
36. Ho, Y. S.; McKay, G. *Process Biochem.* **1999**, 34, 451-465.
-